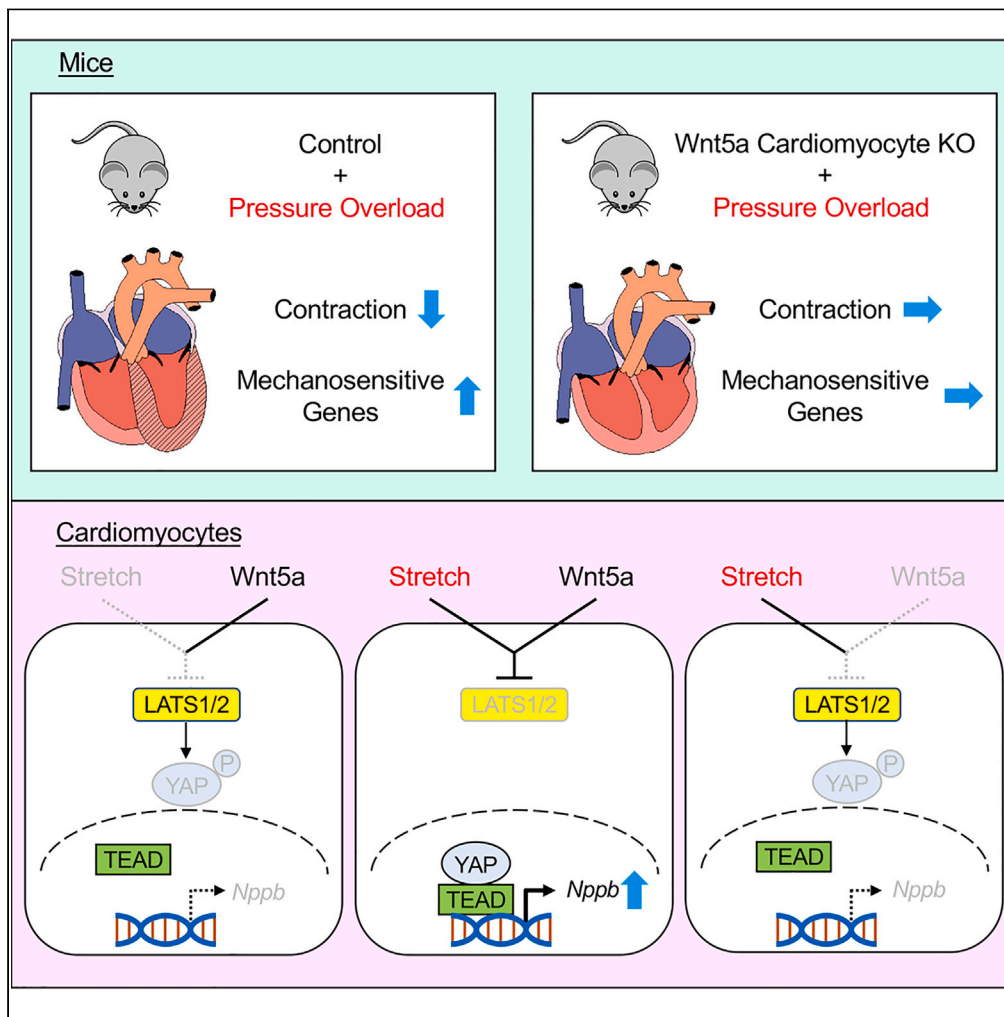


Article

# Wnt5a-YAP signaling axis mediates mechanotransduction in cardiac myocytes and contributes to contractile dysfunction induced by pressure overload



Hiroshi Kishimoto,  
Masayoshi  
Iwasaki, Kensaku  
Wada, ..., Issei  
Komuro, Akira  
Kikuchi, Ichiro  
Shiojima

iwasakim@hirakata.kmu.ac.jp  
(M.I.)  
shiojima@hirakata.kmu.ac.jp  
(I.S.)

**Highlights**

Wnt5a deletion in  
cardiomyocytes  
attenuates TAC-induced  
cardiac dysfunction

Myocyte Wnt5a is  
required for TAC-induced  
upregulation of  
mechanosensitive genes

Wnt5a is required for  
stretch-induced YAP  
nuclear translocation in  
cardiomyocytes

Wnt5a-YAP signaling axis  
mediates  
mechanotransduction in  
cardiac myocytes

Kishimoto et al., iScience 26,  
107146  
July 21, 2023 © 2023 The  
Authors.  
[https://doi.org/10.1016/  
j.isci.2023.107146](https://doi.org/10.1016/j.isci.2023.107146)



## Article

## Wnt5a-YAP signaling axis mediates mechanotransduction in cardiac myocytes and contributes to contractile dysfunction induced by pressure overload

Hiroshi Kishimoto,<sup>1</sup> Masayoshi Iwasaki,<sup>1,\*</sup> Kensaku Wada,<sup>1</sup> Keita Horitani,<sup>1</sup> Osamu Tsukamoto,<sup>2</sup> Kenta Kamikubo,<sup>2</sup> Seitaro Nomura,<sup>3</sup> Shinji Matsumoto,<sup>4</sup> Takeshi Harada,<sup>4</sup> Daisuke Motooka,<sup>5</sup> Daisuke Okuzaki,<sup>5</sup> Seiji Takashima,<sup>2</sup> Issei Komuro,<sup>3</sup> Akira Kikuchi,<sup>4,6</sup> and Ichiro Shiojima<sup>1,7,\*</sup>

## SUMMARY

**Non-canonical Wnt signaling activated by Wnt5a/Wnt11 is required for the second heart field development in mice. However, the pathophysiological role of non-canonical Wnt signaling in the adult heart has not been fully elucidated. Here we show that cardiomyocyte-specific Wnt5a knockout mice exhibit improved systolic function and reduced expression of mechanosensitive genes including *Nppb* when subjected to pressure overload. In cultured cardiomyocytes, Wnt5a knockdown reduced *Nppb* upregulation induced by cyclic cell stretch. Upstream analysis revealed that TEAD1, a transcription factor that acts with Hippo pathway co-activator YAP, was downregulated both *in vitro* and *in vivo* by Wnt5a knockdown/knockout. YAP nuclear translocation was induced by cell stretch and attenuated by Wnt5a knockdown. Wnt5a knockdown-induced *Nppb* downregulation during cell stretch was rescued by Hippo inhibition, and the rescue effect was canceled by knockdown of YAP. These results collectively suggest that Wnt5a-YAP signaling axis mediates mechanotransduction in cardiomyocytes and contributes to heart failure progression.**

## INTRODUCTION

Wnts constitute a large family of cysteine-rich secreted proteins that elicit evolutionarily conserved intracellular signaling and control diverse processes during development.<sup>1</sup> Wnt signaling also plays critical roles in various physiological and pathological processes in adult organisms including stem cell self-renewal/differentiation, degenerative diseases, and carcinogenesis.<sup>2</sup> The initially identified intracellular signaling pathway activated by Wnts was a  $\beta$ -catenin-dependent or canonical pathway. In canonical Wnt pathway, Wnt stimulation induces cytosolic  $\beta$ -catenin stabilization and nuclear translocation, where it binds to T cell factor/Lymphoid enhancer factor (Tcf/Lef) and activates Tcf/Lef-dependent transcription.<sup>2,3</sup> Subsequently  $\beta$ -catenin-independent or non-canonical Wnt pathway was also identified. There are at least two non-canonical Wnt pathways called planar cell polarity (PCP) pathway and  $\text{Ca}^{2+}$  pathway, the former is mediated by small G proteins such as RhoA and Rac and regulates cell polarity and migration whereas the latter is mediated by intracellular  $\text{Ca}^{2+}$  mobilization and stimulates cell migration and inhibits canonical Wnt pathway.<sup>3-5</sup> Wnt5a and Wnt11 are two major Wnt ligands that preferentially activate non-canonical Wnt signaling, although the selectivity of canonical versus non-canonical Wnt signaling appears to be determined by distinct set of receptors rather than the Wnt ligands themselves.<sup>3,6</sup>

Previous studies have shown that canonical Wnt signaling is required for heart development and involved in cardiac hypertrophy and remodeling in the adult.<sup>7,8</sup> It was also reported that non-canonical Wnt signaling is required for normal heart development: inhibition of Wnt11 in frogs disrupts heart formation,<sup>9</sup> and combined deletion of *Wnt5a/Wnt11* genes in mice results in loss of second heart field progenitors and single-chambered heart.<sup>10</sup> However, the pathophysiological role of non-canonical Wnt signaling in the adult heart remains elusive.

<sup>1</sup>Department of Medicine II, Kansai Medical University, Osaka 573-1010, Japan

<sup>2</sup>Department of Medical Biochemistry, Osaka University Graduate School of Medicine, Osaka 565-0871, Japan

<sup>3</sup>Department of Cardiovascular Medicine, Graduate School of Medicine, The University of Tokyo, Tokyo 113-8655, Japan

<sup>4</sup>Department of Molecular Biology and Biochemistry, Osaka University Graduate School of Medicine, Osaka 565-0871, Japan

<sup>5</sup>Genome Information Research Center, Research Institute for Microbial Diseases, Osaka University, Osaka 565-0871, Japan

<sup>6</sup>Center for Infectious Disease Education and Research, Osaka University, Osaka 565-0871, Japan

<sup>7</sup>Lead contact

\*Correspondence: [iwasakim@hirakata.kmu.ac.jp](mailto:iwasakim@hirakata.kmu.ac.jp) (M.I.), [shiojima@hirakata.kmu.ac.jp](mailto:shiojima@hirakata.kmu.ac.jp) (I.S.)

<https://doi.org/10.1016/j.isci.2023.107146>



Here, we show that cardiomyocyte-specific *Wnt5a* knockout mice exhibit improved systolic function and reduced expression of mechanosensitive genes when subjected to pressure overload. We also show that *Wnt5a* mediates mechanotransduction in cardiac myocytes through YAP activation. These results suggest that *Wnt5a*-YAP signaling axis mediates mechanotransduction in cardiac myocytes and contributes to the transition to heart failure.

## RESULTS

### Pressure overload-induced cardiac dysfunction is attenuated in cardiomyocyte-specific *Wnt5a* knockout mice

To explore the pathophysiological role of *Wnt5a* in the adult heart, we generated tamoxifen-inducible *Wnt5a* cardiomyocyte-specific knockout (CKO) mice by crossing *Wnt5a* floxed mice<sup>11</sup> with *Myh6-Cre/Esr1* transgenic mice expressing tamoxifen-inducible Cre under the control of  $\alpha$ -myosin heavy chain promoter<sup>12</sup> (Figure 1A). Intraperitoneal tamoxifen administration (8 mg/kg/day) was started at 12 weeks of age, which resulted in 90% reduction in *Wnt5a* expression level in the heart of CKO mice compared to control mice after 2 weeks of tamoxifen injection (Figure 1B). The expression levels of *Wnt11* in the hearts of CKO mice were comparable to those in control mice (Figure 1B). The expression levels of *Nppa* (encoding atrial natriuretic peptide), *Nppb* (encoding brain natriuretic peptide), and *Ctgf* (encoding connective tissue growth factor) genes that are known to be upregulated in stressed hearts were not significantly different between control and CKO mice (Figure 1C). Echocardiographic parameters both at 2 weeks and 12 months after initial tamoxifen injection were also comparable between control and CKO mice (Figure 1D).

We next performed transverse aortic constriction (TAC) at 2 weeks after initial tamoxifen injection (Figure 2A). At 4 weeks after TAC, *Wnt5a* expression was significantly downregulated in control hearts, and the low levels of *Wnt5a* in CKO hearts remained unchanged (Figure 2B). The expression levels of *Wnt11* were not altered by TAC both in control and CKO hearts (Figure 2B). Echocardiography revealed that chamber dilatation, increased wall thickness, and contractile dysfunction of left ventricle induced by TAC were attenuated in CKO hearts compared to control hearts (Figure 2C). Although the heart weight/body weight ratio was not significantly different between control and CKO hearts 4 weeks after TAC (Figure 2D), histological analysis revealed that TAC-induced cardiomyocyte hypertrophy was significantly reduced in CKO hearts as evidenced by decreased myocyte cross sectional area (CSA) (Figure 2E). Histological analysis also revealed that TAC-induced interstitial fibrosis was attenuated in CKO hearts (Figure 3A), and myocardial capillary density did not differ between control and CKO hearts (Figure 3B). TAC significantly increased the expression levels of *Nppa*, *Nppb*, and *Ctgf* genes, and *Wnt5a* deletion resulted in the reduction of *Nppb* expression levels in response to TAC (Figure 3C). These observations indicate that pressure overload-induced cardiac dysfunction is attenuated in the heart of *Wnt5a* CKO mice.

### Cardiomyocyte-specific *Wnt5a* deletion diminishes the pressure overload-induced upregulation of genes related to “cellular response to mechanical stimuli”

To gain mechanistic insights into how cardiomyocyte-specific *Wnt5a* deletion blunts the response to pressure overload, we carried out RNA-seq analysis for mRNA samples obtained from control and *Wnt5a* CKO hearts at 3 different time points (at the end of tamoxifen treatment, 2 weeks after sham/TAC operation, and 4 weeks after sham/TAC operation). Heatmap of the differentially expressed genes identified 5 clusters of genes whose expression patterns in response to pressure overload were altered by *Wnt5a* deletion in myocytes (Figure 4A and Table S1). The differential expression patterns of genes in each cluster are shown in Figure 4B. For instance, expressions of genes in cluster 1 are downregulated both in 2 weeks and 4 weeks after TAC in control hearts but they are downregulated only at 2 weeks after TAC in CKO hearts. We then focused on genes in “cellular response to mechanical stimuli” category in cluster 2 (Figure 4C). Genes in this cluster are upregulated in control hearts but not in *Wnt5a* CKO hearts both at 2 weeks and 4 weeks after TAC, and these differential expression patterns of genes are consistent with our observation that cardiomyocyte-specific *Wnt5a* deletion blunts the response to pressure overload. Based on the results of RNA-seq analysis, we hypothesized that *Wnt5a* is involved in mechanosensing in cardiac myocytes.

### *Wnt5a* is required for the responses to mechanical stimuli in cardiac myocytes

To test the above-mentioned hypothesis, we performed experiments in neonatal rat ventricular cardiomyocytes (NRVCs) subjected to cyclic stretch, where cultured cardiac myocytes seeded on

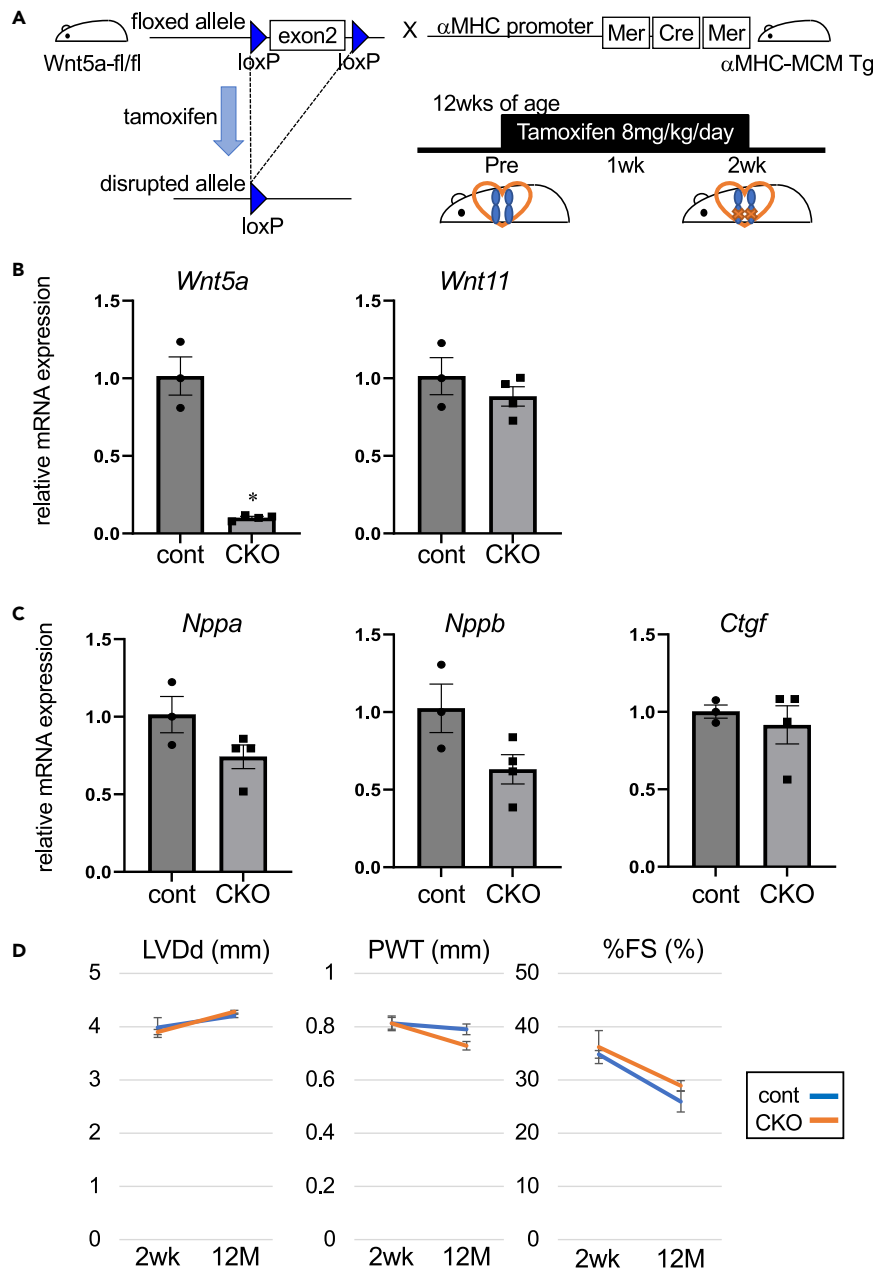


**Figure 1. Generation of cardiomyocyte-specific *Wnt5a* knockout mice**

(A) Schematic illustration depicting generation of cardiac-specific *Wnt5a* knockout mice and the timing of tamoxifen treatment.

(B and C) Relative mRNA levels of *Wnt5a*, *Wnt11*, *Nppa*, *Nppb*, and *Ctgf* at day 14 after initial tamoxifen injection.

\*sp < 0.05 versus cont, n = 3 for cont and n = 4 for CKO.

(D) Echocardiographic evaluation of left ventricular dimension and contraction at 14 days and 12 months after initial tamoxifen injection. LVDd, left ventricular dimension at diastole; PWT, posterior wall thickness; %FS, percentile fractional shortening. n = 4 for cont and n = 3 for CKO.

deformable silicon dishes were uniaxially stretched for 8 h (20% in length, 30 cycles/minute). *Wnt5a* was predominantly expressed in myocyte fraction compared to non-myocyte fraction (Figure 5A), and siRNA-mediated knockdown of *Wnt5a* gene reduced the expression of endogenous *Wnt5a* approximately by 75% (Figure 5B). Cyclic stretch for 8 h significantly upregulated *Nppb* expression levels in NRVCs, and this stretch-induced *Nppb* upregulation was diminished by knockdown of *Wnt5a* (Figure 5C).

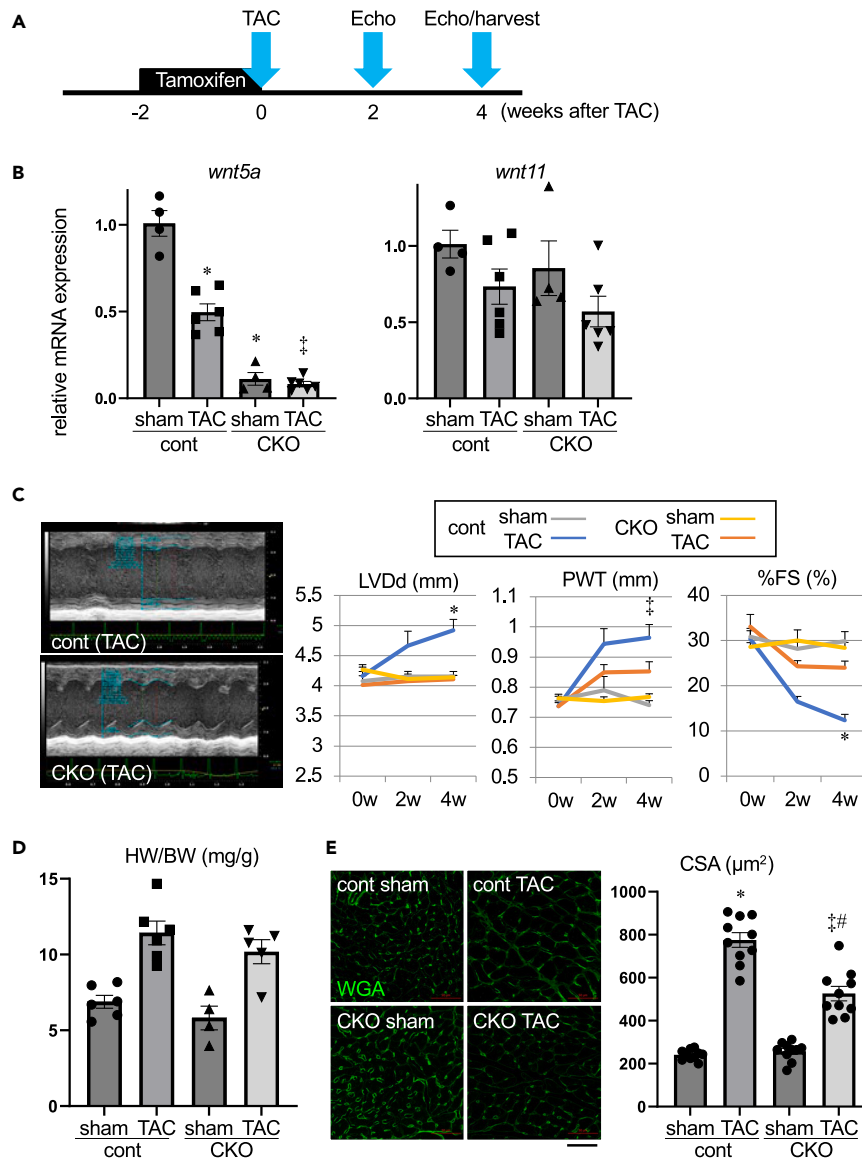


**Figure 2. Pressure overload-induced cardiac dysfunction is attenuated in cardiomyocyte-specific *Wnt5a* knockout mice**

(A) Timeline depicting tamoxifen treatment, transverse aortic constriction (TAC), echocardiography, and tissue harvest. (B) Relative mRNA levels of *Wnt5a* and *Wnt11* at 4 weeks after TAC. \* $p < 0.001$  versus sham-control, † $p < 0.001$  versus TAC-control,  $n = 4, 6, 4,$  and  $6$  for each group. (C) Echocardiographic evaluation of left ventricular dimension and contraction at 2 weeks and 4 weeks after TAC. \* $p < 0.01$  versus other groups, † $p < 0.01$  versus sham-cont and sham-CKO,  $n = 4, 5, 4,$  and  $5$  for each group. (D) Heart weight (HW) (mg)/body weight (BW) (g) ratio at 4 weeks after TAC.  $n = 6, 6, 4,$  and  $5$  for each group. (E) Cross sectional area (CSA) of myocytes at 4 weeks after TAC. Left panel shows the wheat germ agglutinin (WGA) staining of sarcolemma. Scale bar,  $50\mu\text{m}$ . \* $p < 0.001$  versus sham-cont, † $p < 0.001$  versus sham-CKO, # $p < 0.001$  versus TAC-cont.  $n = 10$  for each group.

Treatment of cultured NRVCs with recombinant *Wnt5a* protein<sup>13</sup> induced Dishevelled2 (Dvl2) phosphorylation at the concentration of 100 and 200 ng/mL as indicated by reduced electrophoretic mobility (Figure 5D). However, supplementation of *Wnt5a* protein (100 and 200 ng/mL) did not increase but rather decreased *Nppb* expression following cyclic stretch (Figure 5E). These observations suggest that *Wnt5a* is required for but does not enhance mechanotransduction-like responses in cardiac myocytes.

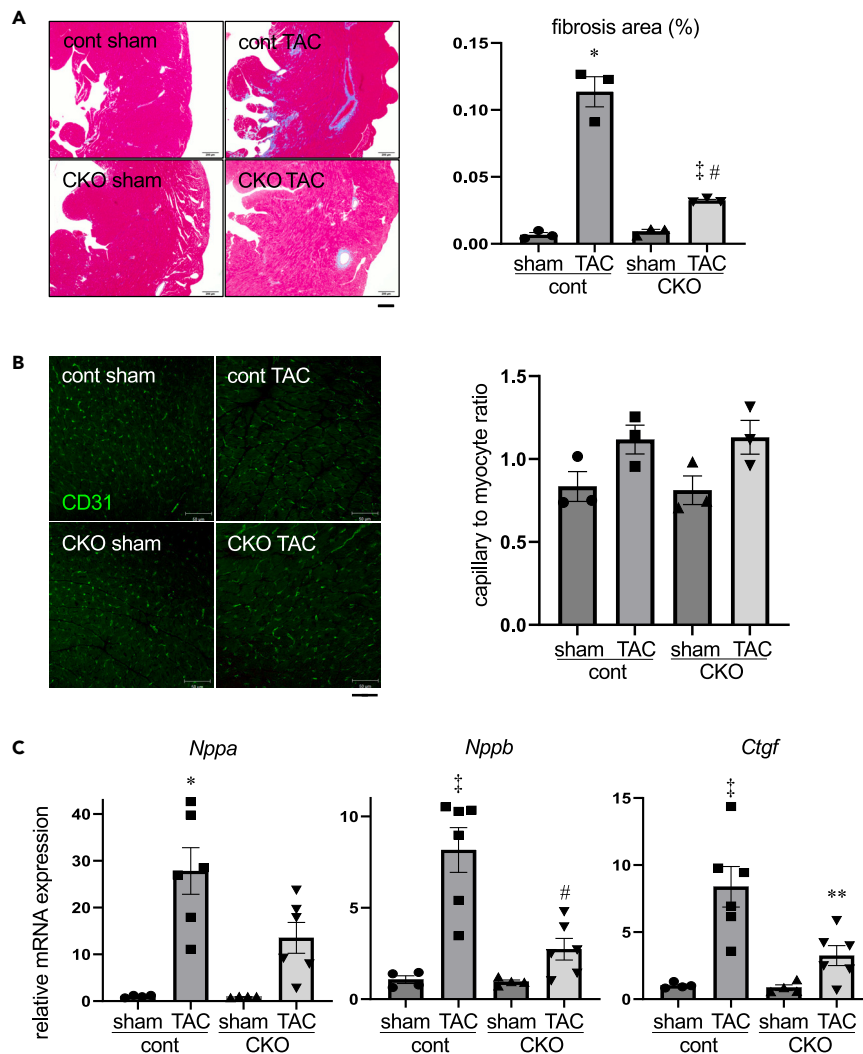


**Figure 3. Pressure overload-induced cardiac fibrosis and stress-responsive gene expression are attenuated in cardiomyocyte-specific *Wnt5a* knockout mice**

(A) Interstitial fibrosis at 4 weeks after TAC. Left panel shows the Masson's trichrome staining of connective tissues. Right panel shows the relative fibrosis area. Scale bar, 200 $\mu$ m. \* $p < 0.001$  versus sham-cont, ‡ $p < 0.05$  versus sham-CKO, # $p < 0.001$  versus TAC-cont.  $n = 3$  for each group.

(B) Capillaries in the myocardium 4 weeks after TAC. Left panel shows the CD31 staining of capillaries. Right panel shows capillary to myocyte ratio. Scale bar, 50 $\mu$ m.  $n = 3$  for each group.

(C) Relative mRNA levels of *Nppa*, *Nppb*, and *Ctgf* at 4 weeks after TAC. \* $p < 0.05$  versus sham-cont, ‡ $p < 0.001$  versus sham-cont, # $p < 0.001$  versus TAC-cont, \*\* $p < 0.005$  versus TAC-cont.  $n = 4, 6, 4,$  and  $6$  for each group.

### ***Wnt5a* mediates mechanotransduction in cardiac myocytes through YAP activation**

To examine the mechanism by which *Wnt5a* mediates mechanotransduction in cardiomyocytes, we carried out RNA-seq analysis in NRVCs. Principal component analysis demonstrated that siRNA-mediated knockdown of *Wnt5a* affected a large scale of transcriptional regulation in NRVCs at baseline before cyclic stretch (Figure 6A, blue squares versus orange circles), and the contribution of PC1 to changes in gene expression levels because of cyclic stretch was relatively small in the *Wnt5a* knockdown group (Figure 6A, compare the changes from blue squares to purple crosses with those from orange circles to green triangles). Moreover, pathway analysis suggested that *Wnt5a* knockdown significantly downregulated transcription factor binding in NRVCs compared to control cells after 8 h of cell stretch (Table S2). We therefore carried out upstream analysis of transcription factors and found that *Wnt5a* knockdown inhibited 15 transcription factors in NRVCs during 8 h of cyclic stretch (Table S3). We also performed upstream analysis of transcription

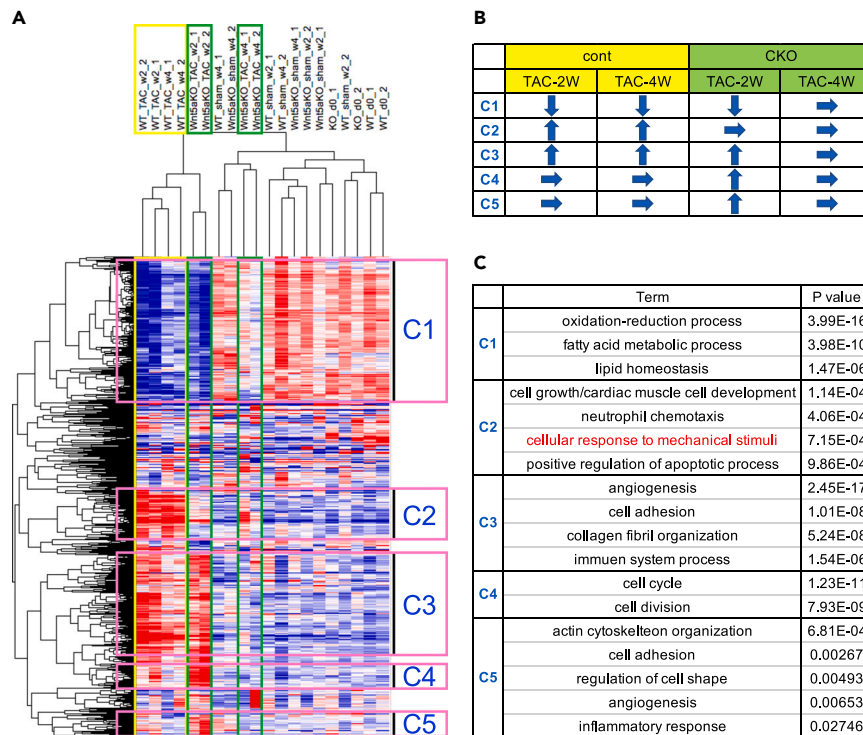


**Figure 4. Cardiac myocyte-specific *Wnt5a* deletion diminishes the pressure overload-induced upregulation of genes related to "cellular response to mechanical stimuli"**

(A) Heatmap of RNA-seq transcriptome analysis showing differentially expressed genes between TAC-cont and TAC-CKO at 2 and 4 weeks after the operation by hierarchical clustering analysis. Yellow rectangles show TAC-cont, green rectangles show TAC-CKO, and gene clusters are shown by pink rectangles.

(B) Schematic illustration of the expression patterns of genes in 5 clusters.

(C) Gene ontology terms of differentially expressed genes in 5 clusters. Gene names in each gene ontology term are shown in Table S1. Gene names in each GO term are shown in Table S1.

factors in the hearts and found that 9 transcription factors were inhibited in *Wnt5a* CKO hearts compared to control hearts (Table S4). When we compared the results of upstream analysis of transcription factors between *in vivo* and *in vitro* experiments, TEA domain transcription factors 1 (TEAD1) was the only transcription factor inhibited in both settings (Tables S3, S4, and Figure 6B). TEAD regulates gene expression through interaction with yes-associated protein (YAP) and its paralog, transcriptional coactivator with a PDZ-binding motif (TAZ).<sup>14</sup> YAP/TAZ is a transcriptional co-activator in the Hippo pathway, and Mst1/2-Lats1/2 kinase cascade phosphorylates YAP/TAZ to induce its cytoplasmic retention and inhibition of YAP/TAZ activity.<sup>14</sup> Consistently, YAP1 activity was shown to be downregulated by *Wnt5a* deletion in NRVCs (Table S3). Moreover, *Wnt5a* was previously shown to activate YAP/TAZ.<sup>15–17</sup> Based on these data and previous reports, we hypothesized that *Wnt5a* mediates mechanotransduction in cardiac myocytes through YAP activation.

To test this hypothesis, nuclear localization of YAP after cyclic stretch was examined in NRVCs. Western blot analysis of NRVC nuclear extracts revealed that cyclic stretch induced nuclear translocation of YAP in control cells but not in *Wnt5a* knockdown cells (Figure 6C, left panel). In western blot analysis of NRVC whole cell lysate, total protein amount of YAP was increased by cyclic stretch in control cells but not in *Wnt5a* knockdown cells (Figure 6C, right panel). YAP immunostaining also revealed stretch-induced nuclear retention of YAP in control cells but not in *Wnt5a* knockdown cells (Figure 6D). These results indicate that cyclic stretch in NRVCs induces nuclear retention of YAP in a *Wnt5a*-dependent manner.

To test whether YAP is involved in mechanotransduction in cardiac myocytes, the effect of *Yap1* knockdown in NRVCs was examined. siRNA-mediated knockdown of *Yap1* gene reduced the expression of endogenous *Yap1* approximately by 80% (Figure 6E). Upregulation of *Nppb* gene in NRVCs induced by cyclic

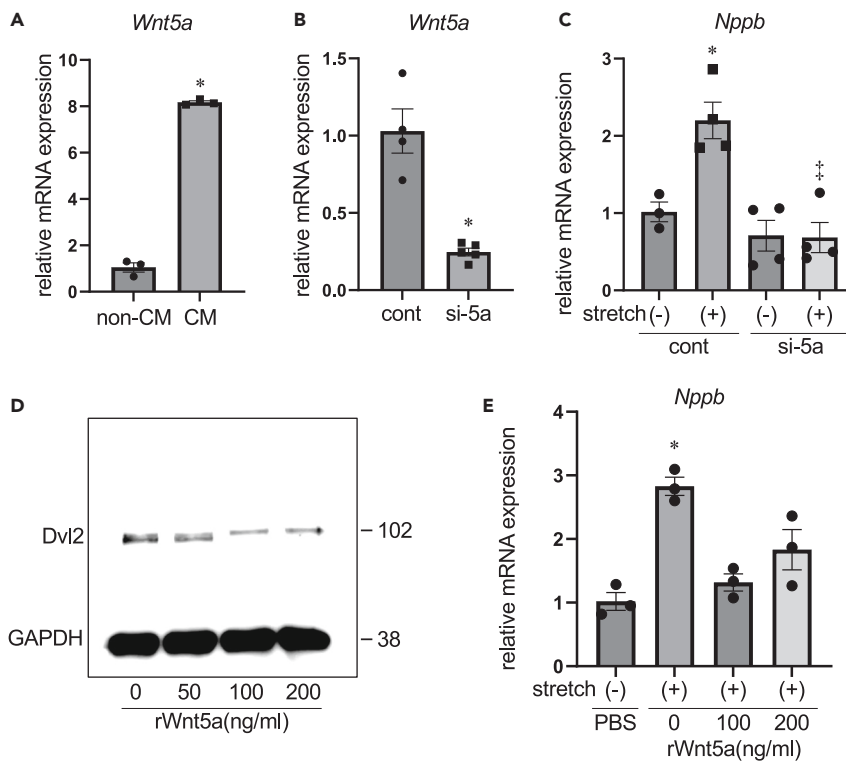


**Figure 5. Wnt5a is required for the responses to mechanical stimuli in cardiac myocytes**

(A) Relative mRNA levels of *Wnt5a* in cardiomyocyte (CM) fraction and non-CM fraction. \* $p < 0.01$  versus non-CM.  $n = 3$  for each group.

(B) Relative mRNA levels of *Wnt5a* in cardiac myocytes following siRNA-mediated *Wnt5a* knockdown. \* $p < 0.05$  versus cont.  $n = 4$  for cont and  $n = 5$  for si-*Wnt5a* (si-5a).

(C) Relative mRNA levels of *Nppb* in cardiac myocytes after 8 h of cyclic stretch. \* $p < 0.005$  versus stretch (-)-cont, † $p < 0.001$  versus stretch (+)-cont.  $n = 3, 4, 4,$  and  $4$  for each group.

(D) Western blot analysis of Disheveled2 (Dvl2) in cardiac myocytes treated with recombinant *Wnt5a* protein (50, 100, and 200 ng/mL) for 3 h.

(E) Relative mRNA levels of *Nppb* in cardiac myocytes treated with recombinant *Wnt5a* protein (100 and 200 ng/mL) during 8 h of stretch. \* $p < 0.005$  versus stretch (-)-cont.  $n = 3$  for each group.

stretch was attenuated by *Yap1* knockdown (Figure 6F), indicating that stretch-induced *Nppb* upregulation is dependent on YAP. To further confirm that *Wnt5a*-YAP signaling axis mediates mechanotransduction in cardiac myocytes, we attempted to activate YAP independently of *Wnt5a* in NRVCs. For this purpose, we used XMU-MP-1, which pharmacologically inhibits Mst1/2 kinases and thereby promotes YAP nuclear translocation.<sup>18</sup> *Wnt5a* knockdown attenuated cyclic stretch-induced *Nppb* upregulation, and XMU-MP1 treatment reversed this inhibitory effect of *Wnt5a* knockdown, suggesting that *Wnt5a* signaling affects *Nppb* expression upstream or independently of Mst1/2. Of note, this upregulation of *Nppb* expression induced by XMU-MP-1 in *Wnt5a* knockdown cells was canceled by additional knockdown of *Yap1* (Figure 6G). Collectively, these results suggest that *Wnt5a* mediates mechanotransduction in cardiomyocytes through YAP activation.

## DISCUSSION

In the present study we explored the pathophysiological role of cardiomyocyte-derived *Wnt5a* in the adult heart and found that (i) *Wnt5a* CKO mice exhibit improved systolic function in response to pressure overload and (ii) *Wnt5a* mediates cell stretch-induced upregulation of *Nppb* in cultured cardiac myocytes through activation of transcriptional co-factor YAP. These findings suggest that non-canonical *Wnt5a*-YAP signaling axis mediates mechanotransduction in cardiac myocytes and contributes to the transition to heart failure in response to pressure overload.



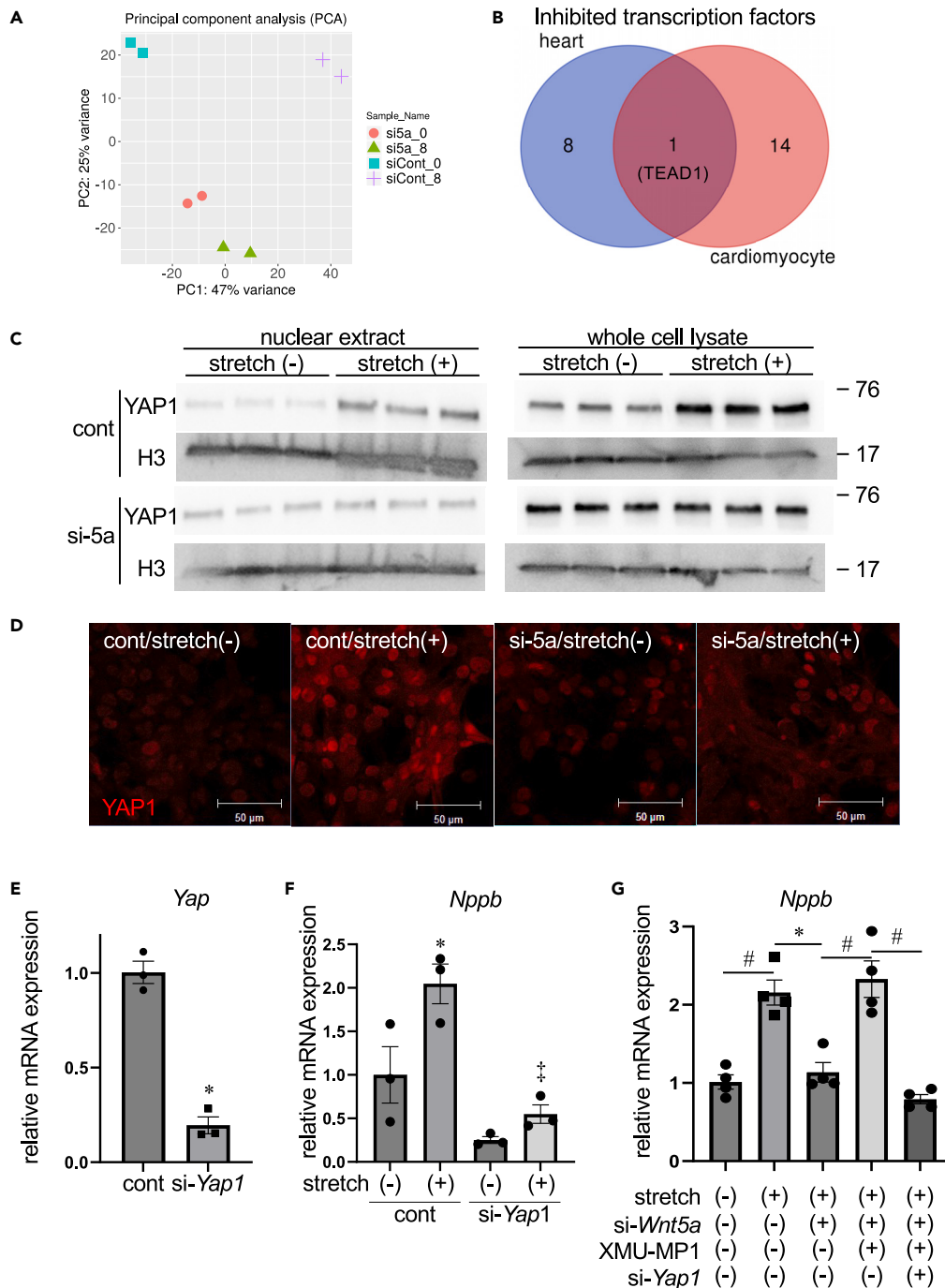


**Figure 6. Wnt5a mediates mechanotransduction in cardiac myocytes through YAP activation**

(A) Principal component analysis of control and *Wnt5a*-knocked down cardiac myocytes at baseline and 8 h after stretch.

(B) Venn diagram showing the number of shared and exclusive transcription factors downregulated by *Wnt5a* knockout in the heart (blue) and *Wnt5a* knockdown in cultured cardiac myocytes (orange). See also Tables S3 and S4.

(C) Western blot analysis of YAP in nuclear extract (left) and whole cell lysate (right) in cultured cardiac myocytes.

(D) Immunohistochemistry of YAP1 in cultured cardiac myocytes. Scale bar, 50  $\mu$ m.

(E) Relative mRNA levels of *Yap1* in cardiac myocytes following siRNA-mediated *Yap1* knockdown. \*p < 0.01 versus cont. n = 6 for each group.

(F) Relative mRNA levels of *Nppb* in cardiac myocytes. \*p < 0.05 versus stretch (-)-cont,  $\ddagger$ p < 0.005 versus stretch (+)-cont. n = 3 for each group.

(G) Relative mRNA levels of *Nppb* in cardiac myocytes. #p < 0.01, \*p < 0.05. n = 4 for each group.

### Wnt5a-YAP signaling axis mediates mechanotransduction in cardiac myocytes

The ability of cells to respond to the alterations in external physical stimuli is crucial for the maintenance of tissues such as muscle and bone that are exposed to varying degrees of mechanical stress.<sup>19</sup> YAP was originally identified as a protein that associates with Src family of tyrosine kinase Yes. Subsequently YAP was shown to act as a co-activator of TEAD family of transcription factors downstream of Hippo signaling pathway, where upstream kinase MST1/2 phosphorylates and activates LATS1/2, which in turn phosphorylates and inactivates YAP by inducing cytoplasmic retention and proteasome-dependent degradation.<sup>14</sup> It was also shown that YAP is an effector of cellular mechanosensing pathway and translocates to the nucleus in response to various mechanical stimuli.<sup>20</sup> Furthermore, it was also shown that Wnt5a activates YAP in a  $\beta$ -catenin-independent but LATS1/2-dependent fashion,<sup>16</sup> collectively suggesting the possibility that Wnt5a-YAP signaling axis is involved in cellular responses to mechanical stimuli. However, to the best of our knowledge, this is the first report demonstrating that endogenous Wnt5a mediates mechanotransduction through YAP activation. Wnt5a was necessary for the activation of YAP and the upregulation of *Nppb* gene expression in response to cell stretch in cardiac myocytes. However, treatment with Wnt5a protein did not increase but rather decreased *Nppb* expression in the presence of cyclic stretch. Although the precise reasons for such apparent discrepancies are not clear at present, we speculate that appropriate levels of Wnt5a signaling may be required for the integrity of mechanosensing apparatus, and that both reduced and enhanced Wnt5a signaling may result in the impairment of mechanotransduction and YAP activation. The exact mechanistic basis for Wnt5a-mediated mechanotransduction remains to be elucidated.

### Cardiomyocyte-derived Wnt5a contributes to the transition to heart failure in response to pressure overload

In this study we show that *Wnt5a* CKO mice exhibit improved systolic function in response to pressure overload, suggesting that cardiomyocyte-derived Wnt5a contributes to heart failure progression. Although the precise mechanism for Wnt5a-mediated cardiac dysfunction is not clear at present, we speculate that activation of mechanosensitive genes contributes to the progression of heart failure following pressure overload. Responses of the heart to increased load is generally recognized as adaptive processes. However, sustained mechanical stress results in maladaptive responses of the heart, leading to adverse remodeling and contractile dysfunction of the heart.<sup>21</sup> Thus, it is possible that appropriate levels of reduction in mechanosensation and mechanoreponse inhibits or delays the transition from adaptive to maladaptive cardiac hypertrophy following pressure overload. Of note, it was previously reported that neutrophil-specific *Wnt5a* deletion also protects the heart from pressure overload-induced dysfunction,<sup>22</sup> suggesting that Wnt5a derived from both myocytes and non-myocytes plays a significant role in heart failure progression.

YAP is a downstream effector of Hippo pathway, and several studies have investigated the role of Hippo signaling in pressure overload-induced heart failure. Cardiac-specific homozygous deletion of YAP results in dilated cardiomyopathy-like phenotype at baseline and heterozygous cardiac-specific YAP knockout mice exhibit exacerbated contractile dysfunction after TAC, suggesting that YAP is cardioprotective.<sup>23</sup> However, YAP activation by cardiac-specific deletion of *WW45* (also called *Salvador*), a scaffold protein required for LATS1/2 activation by MST1/2, results in enhanced contractile dysfunction after TAC, suggesting that YAP activation in this case is deleterious for the heart.<sup>24</sup> Moreover, although both inactivation (heterozygous deletion of YAP) and activation (homozygous deletion of *WW45*) of YAP promotes heart failure in response to pressure overload, combined deletion of YAP (heterozygous) and *WW45* (homozygous) in cardiac myocytes is protective against pressure overload-induced cardiac dysfunction.<sup>24</sup> These results collectively suggest that YAP must be maintained at appropriate levels for the heart to maintain normal function. It is therefore possible that pressure overload-induced YAP activation is decreased by *Wnt5a* deletion to “appropriate levels for the heart”, leading to maintained contractile function in response to pressure overload. Future studies will elucidate how mechanotransduction mediated by Wnt5a-YAP signaling axis contributes to the regulation of cardiac function.

There are some discrepancies between our present study and several previous literature. Although we found that *Wnt5a* gene expression is downregulated in response to pressure overload (Figure 1B), it was previously reported that Wnt5a is upregulated in the myocardium of patients with heart failure and in the heart of mice following TAC.<sup>25,26</sup> The precise reasons for such discrepancies are not clear at present. On the other hand, consistent with our present study, it was previously reported that simultaneous *in vivo* knockdown of *Wnt5a* and *Wnt11* using shRNA-*Wnt5a*/*Wnt11*-AAV9 vector exhibits cardioprotective effects (e.g., improved contraction and reduced fibrosis) after TAC.<sup>26</sup> However, it should be noted that *in vivo*

knockdown by shRNA vectors affect all cell types in the heart whereas *Wnt5a* gene was knocked out in a cardiomyocyte-specific manner in the present study.

### Limitations of the study

Several limitations exist in the present study. First, although we were able to show that *Wnt5a* is necessary to activate YAP and induce *Nppb* gene expression in response to cell stretch, the detailed mechanistic basis for *Wnt5a*-mediated mechanotransduction remains unresolved. Second, the observation that *Wnt5a* CKO mice exhibit improved systolic function and reduced expression of mechanosensitive genes in response to pressure overload does not directly demonstrate that reduced mechanotransduction signaling induced by *Wnt5a* knockout plays a causal role in functional improvement. It is also possible that other *Wnt5a*-mediated signaling plays a role in pressure overload-induced contractile dysfunction.

### STAR★METHODS

Detailed methods are provided in the online version of this paper and include the following:

- KEY RESOURCES TABLE
- RESOURCE AVAILABILITY
  - Lead contact
  - Materials availability
  - Data and code availability
- EXPERIMENTAL MODEL AND STUDY PARTICIPANT DETAILS
  - Animals
- METHODS DETAILS
  - Transverse aortic constriction (TAC) and echocardiography
  - Quantitative real-time PCR (qRT-PCR)
  - Histological analysis
  - RNA-seq analysis
  - Preparation of neonatal rat cardiac myocytes
  - Cyclic stretch of cultured cardiac myocytes
  - siRNA-mediated knockdown and *Wnt5a* stimulation
  - Western blot analysis
  - Immunocytochemistry
- QUANTIFICATION AND STATISTICAL ANALYSIS

### SUPPLEMENTAL INFORMATION

Supplemental information can be found online at <https://doi.org/10.1016/j.isci.2023.107146>.

### ACKNOWLEDGMENTS

We thank Yoshiko Karatsu for technical assistance and Tomoki Kitawaki for advices in statistical analyses. This work was supported by Grant-in-Aid for Scientific Research (18H02814) from the Japan Society for the Promotion of Science.

### AUTHOR CONTRIBUTIONS

Conceptualization, M.I. and I.S.; Investigation, H.K, M.I., K.W., and K.H.; Resources, O.T, K.K., S.M., T.H., S.T., and A.K.; Formal Analysis, S.N, D.M., D.O., and I.K.; Writing – Original Draft, H.K, M.I., and I.S.; Writing – Review and Editing, M.I., S.N., O.D., A.K., and I.S.; Visualization, H.K, M.I., K.H., S.N., and I.S.; Supervision, M.I. and I.S.; Funding Acquisition, I.S.

### DECLARATION OF INTERESTS

The authors declare no competing interests.

Received: September 7, 2022

Revised: March 31, 2023

Accepted: June 12, 2023

Published: June 15, 2023

## REFERENCES

- Clevers, H. (2006). Wnt/beta-catenin signaling in development and disease. *Cell* 127, 469–480. <https://doi.org/10.1016/j.cell.2006.10.018>.
- Nusse, R., and Clevers, H. (2017). Wnt/beta-Catenin Signaling, Disease, and Emerging Therapeutic Modalities. *Cell* 169, 985–999. <https://doi.org/10.1016/j.cell.2017.05.016>.
- Kikuchi, A., Yamamoto, H., and Sato, A. (2009). Selective activation mechanisms of Wnt signaling pathways. *Trends Cell Biol.* 19, 119–129. <https://doi.org/10.1016/j.tcb.2009.01.003>.
- Kikuchi, A., Yamamoto, H., Sato, A., and Matsumoto, S. (2012). Wnt5a: its signalling, functions and implication in diseases. *Acta Physiol.* 204, 17–33. <https://doi.org/10.1111/j.1748-1716.2011.02294.x>.
- Nishita, M., Enomoto, M., Yamagata, K., and Minami, Y. (2010). Cell/tissue-tropic functions of Wnt5a signaling in normal and cancer cells. *Trends Cell Biol.* 20, 346–354. <https://doi.org/10.1016/j.tcb.2010.03.001>.
- van Amerongen, R., Mikels, A., and Nusse, R. (2008). Alternative wnt signaling is initiated by distinct receptors. *Sci. Signal.* 1, re9. <https://doi.org/10.1126/scisignal.135re9>.
- Gessert, S., and Kühl, M. (2010). The multiple phases and faces of wnt signaling during cardiac differentiation and development. *Circ. Res.* 107, 186–199. <https://doi.org/10.1161/CIRCRESAHA.110.221531>.
- Bergmann, M.W. (2010). WNT signaling in adult cardiac hypertrophy and remodeling: lessons learned from cardiac development. *Circ. Res.* 107, 1198–1208. <https://doi.org/10.1161/CIRCRESAHA.110.223768>.
- Pandur, P., Läsche, M., Eisenberg, L.M., and Kühl, M. (2002). Wnt-11 activation of a non-canonical Wnt signalling pathway is required for cardiogenesis. *Nature* 418, 636–641. <https://doi.org/10.1038/nature00921>.
- Cohen, E.D., Miller, M.F., Wang, Z., Moon, R.T., and Morrisey, E.E. (2012). Wnt5a and Wnt11 are essential for second heart field progenitor development. *Development* 139, 1931–1940. <https://doi.org/10.1242/dev.069377>.
- Sato, A., Kayama, H., Shojima, K., Matsumoto, S., Koyama, H., Minami, Y., Nojima, S., Morii, E., Honda, H., Takeda, K., and Kikuchi, A. (2015). The Wnt5a-Ror2 axis promotes the signaling circuit between interleukin-12 and interferon-gamma in colitis. *Sci. Rep.* 5, 10536. <https://doi.org/10.1038/srep10536>.
- Sohal, D.S., Nghiem, M., Crackower, M.A., Witt, S.A., Kimball, T.R., Tymitz, K.M., Penninger, J.M., and Molkentin, J.D. (2001). Temporally regulated and tissue-specific gene manipulations in the adult and embryonic heart using a tamoxifen-inducible Cre protein. *Circ. Res.* 89, 20–25. <https://doi.org/10.1161/hh1301.092687>.
- Kurayoshi, M., Yamamoto, H., Izumi, S., and Kikuchi, A. (2007). Post-translational palmitoylation and glycosylation of Wnt-5a are necessary for its signalling. *Biochem. J.* 402, 515–523. <https://doi.org/10.1042/BJ20061476>.
- Meng, Z., Moroishi, T., and Guan, K.L. (2016). Mechanisms of Hippo pathway regulation. *Genes Dev.* 30, 1–17. <https://doi.org/10.1101/gad.274027.115>.
- Feng, Y., Liang, Y., Zhu, X., Wang, M., Gui, Y., Lu, Q., Gu, M., Xue, X., Sun, X., He, W., et al. (2018). The signaling protein Wnt5a promotes TGFbeta1-mediated macrophage polarization and kidney fibrosis by inducing the transcriptional regulators Yap/Taz. *J. Biol. Chem.* 293, 19290–19302. <https://doi.org/10.1074/jbc.RA118.005457>.
- Park, H.W., Kim, Y.C., Yu, B., Moroishi, T., Mo, J.S., Plouffe, S.W., Meng, Z., Lin, K.C., Yu, F.X., Alexander, C.M., et al. (2015). Alternative Wnt Signaling Activates YAP/TAZ. *Cell* 162, 780–794. <https://doi.org/10.1016/j.cell.2015.07.013>.
- Luo, C., Balsa, E., Perry, E.A., Liang, J., Tavares, C.D., Vazquez, F., Widlund, H.R., and Puigserver, P. (2020). H3K27me3-mediated PGC1alpha gene silencing promotes melanoma invasion through WNT5A and YAP. *J. Clin. Invest.* 130, 853–862. <https://doi.org/10.1172/JCI130038>.
- Fan, F., He, Z., Kong, L.L., Chen, Q., Yuan, Q., Zhang, S., Ye, J., Liu, H., Sun, X., Geng, J., et al. (2016). Pharmacological targeting of kinases MST1 and MST2 augments tissue repair and regeneration. *Sci. Transl. Med.* 8, 352ra108. <https://doi.org/10.1126/scitranslmed.aaf2304>.
- Jaalouk, D.E., and Lammerding, J. (2009). Mechanotransduction gone awry. *Nat. Rev. Mol. Cell Biol.* 10, 63–73. <https://doi.org/10.1038/nrm2597>.
- Pancieria, T., Azzolin, L., Cordenonsi, M., and Piccolo, S. (2017). Mechanobiology of YAP and TAZ in physiology and disease. *Nat. Rev. Mol. Cell Biol.* 18, 758–770. <https://doi.org/10.1038/nrm.2017.87>.
- Opie, L.H., Commerford, P.J., Gersh, B.J., and Pfeffer, M.A. (2006). Controversies in ventricular remodelling. *Lancet* 367, 356–367. [https://doi.org/10.1016/s0140-6736\(06\)68074-4](https://doi.org/10.1016/s0140-6736(06)68074-4).
- Wang, Y., Sano, S., Oshima, K., Sano, M., Watanabe, Y., Katanasaka, Y., Yura, Y., Jung, C., Anzai, A., Swirski, F.K., et al. (2019). Wnt5a-Mediated Neutrophil Recruitment Has an Obligatory Role in Pressure Overload-Induced Cardiac Dysfunction. *Circulation* 140, 487–499. <https://doi.org/10.1161/CIRCULATIONAHA.118.038820>.
- Byun, J., Del Re, D.P., Zhai, P., Ikeda, S., Shirakabe, A., Mizushima, W., Miyamoto, S., Brown, J.H., and Sadoshima, J. (2019). Yes-associated protein (YAP) mediates adaptive cardiac hypertrophy in response to pressure overload. *J. Biol. Chem.* 294, 3603–3617. <https://doi.org/10.1074/jbc.RA118.006123>.
- Ikeda, S., Mizushima, W., Sciarretta, S., Abdellatif, M., Zhai, P., Mukai, R., Fefelova, N., Oka, S.I., Nakamura, M., Del Re, D.P., et al. (2019). Hippo Deficiency Leads to Cardiac Dysfunction Accompanied by Cardiomyocyte Dedifferentiation During Pressure Overload. *Circ. Res.* 124, 292–305. <https://doi.org/10.1161/CIRCRESAHA.118.314048>.
- Abraityte, A., Vinge, L.E., Askevold, E.T., Lekva, T., Michelsen, A.E., Ranheim, T., Alfsnes, K., Fiane, A., Aakhus, S., Lunde, I.G., et al. (2017). Wnt5a is elevated in heart failure and affects cardiac fibroblast function. *J. Mol. Med.* 95, 767–777. <https://doi.org/10.1007/s00109-017-1529-1>.
- Zou, Y., Pan, L., Shen, Y., Wang, X., Huang, C., Wang, H., Jin, X., Yin, C., Wang, Y., Jia, J., et al. (2021). Cardiac Wnt5a and Wnt11 promote fibrosis by the crosstalk of FZD5 and EGFR signaling under pressure overload. *Cell Death Dis.* 12, 877. <https://doi.org/10.1038/s41419-021-04152-2>.
- deAlmeida, A.C., van Oort, R.J., and Wehrens, X.H. (2010). Transverse aortic constriction in mice. *J. Vis. Exp.* <https://doi.org/10.3791/1729>.
- de Hoon, M.J.L., Imoto, S., Nolan, J., and Miyano, S. (2004). Open source clustering software. *Bioinformatics* 20, 1453–1454. <https://doi.org/10.1093/bioinformatics/bth078>.
- Saldanha, A.J. (2004). Java Treeview—extensible visualization of microarray data. *Bioinformatics* 20, 3246–3248. <https://doi.org/10.1093/bioinformatics/bth349>.
- Huang, D.W., Sherman, B.T., and Lempicki, R.A. (2009). Systematic and integrative analysis of large gene lists using DAVID bioinformatics resources. *Nat. Protoc.* 4, 44–57. <https://doi.org/10.1038/nprot.2008.211>.

## STAR★METHODS

### KEY RESOURCES TABLE

REAGENT or RESOURCE	SOURCE	IDENTIFIER
<b>Antibodies</b>		
CD31	BioLegend	Cat# 102414; RRID: AB_493408
Dvl2	CST	Cat# 3216; RRID: AB_2093338
GAPDH	CST	Cat# 2118; RRID: AB_561053
Histone H3	CST	Cat# 4499; RRID: AB_10544537
YAP	CST	Cat# 14074; RRID: AB_2650491
<b>Chemicals</b>		
tamoxifen	SIGMA	Cat# T5648
wheat germ agglutinin	Invitrogen	W11261
XMU-MP-1 hydrochloride	SIGMA	SML2233
<b>Deposited Data</b>		
Raw and processed RNA-seq data	This paper	GEO: GSE200667
<b>Experimental models: organisms/strains</b>		
Mouse: <i>Wnt5a</i> <sup>fl<sup>ox</sup></sup>	(Sato et al. <sup>11</sup> )	N/A
Mouse: <i>Myh6-Cre/Esr1</i> <sup>T<sup>g</sup></sup>	JACKSON	#005657
<b>Oligonucleotides and siRNA</b>		
Primers and siRNA sequences are listed in <a href="#">Table S5</a>	This paper	N/A
<b>Software and algorithms</b>		
cellSens standard 1.11	OLYMPUS	N/A
Image J bundled with Java 1.8.0	NIH	N/A
ZEN	ZEISS	N/A

### RESOURCE AVAILABILITY

#### Lead contact

Further information and requests for resources and reagents should be directed to the lead contact, Ichiro Shiojima ([shiojima@hirakata.kmu.ac.jp](mailto:shiojima@hirakata.kmu.ac.jp)).

#### Materials availability

This study did not generate new unique reagents.

#### Data and code availability

- Raw and processed RNAseq data have been deposited at Gene Expression Omnibus (<https://www.ncbi.nlm.nih.gov/geo/>). Accession number is listed in the [key resources table](#).
- This manuscript does not report original code.
- Any additional information required to reanalyze the data reported in this paper is available from the [lead contact](#) upon request.

### EXPERIMENTAL MODEL AND STUDY PARTICIPANT DETAILS

#### Animals

*Wnt5a* floxed mice (*Wnt5a*<sup>fl/fl</sup>)<sup>11</sup> and *Myh6-Cre/Esr1* transgenic mice<sup>12</sup> were housed and genotyped with primers listed in [Table S5](#). To generate cardiomyocyte-specific *Wnt5a* knockout mice, *Wnt5a* floxed mice were crossed with *Myh6-Cre/Esr1* transgenic mice, and *Wnt5a*<sup>fl/fl</sup>; *Myh6-Cre/Esr1*<sup>T<sup>g</sup></sup> (*Wnt5a* CKO)

mice and *Wnt5a*<sup>fl/fl</sup> (control) mice were treated with intraperitoneal injection of tamoxifen (8 mg/kg/day) for 14 days beginning at 12 weeks of age. Transverse aortic constriction (TAC) was performed in male mice at 14 weeks of age. All experimental procedures involving mice were approved by the Institutional Animal Care and Use Committee (IACUC) at Kansai Medical University (21–108).

## METHODS DETAILS

### Transverse aortic constriction (TAC) and echocardiography

TAC was performed essentially as described<sup>27</sup> except that a 27 gauge needle was used in this study. For echocardiography we used the Vevo 2100 High Resolution Imaging system (VisualSonics, Toronto, Canada) with a 15–50 MHz transducer mounted on an integrated rail system. Mice were anesthetized using 2–3% isoflurane and moved to a biofeedback warming station that measured heart rate. Standard imaging planes, M-mode, and functional calculations were obtained according to American Society of Echocardiography guidelines. The LV parasternal short-axis view was used to derive fractional shortening, ejection fraction, and ventricular dimensions.

### Quantitative real-time PCR (qRT-PCR)

Total RNA was extracted using RNeasy Mini-kit (QIAGEN), and concentration and quality of extracted RNA was determined by Spectrophotometer ND-1000 (Nano Drop). cDNA was prepared using SuperScript III reverse transcriptase (Invitrogen). qRT-PCR was performed using the SYBR green PCR Kit (QIAGEN) and the Rotor Gene Q machine.  $\beta$ -actin gene was used as an internal control. Primers for qRT-PCR are listed in Table S5.

### Histological analysis

Hearts were fixed in 4% paraformaldehyde, embedded either in paraffin or OCT compound. Sections were stained with Masson's trichrome for detection of fibrosis, Alexa Fluor 488-conjugated wheat germ agglutinin to evaluate cross sectional area of myocytes, and Alexa Fluor 488-conjugated CD31 to measure capillary density.

### RNA-seq analysis

Total RNA was extracted using miRNeasy Mini Kit (QIAGEN), and library was prepared using a TruSeq Stranded mRNA sample preparation kit (Illumina, San Diego, CA). For heart tissues, sequencing was performed on HiSeq 2500 platform in a 75-base single-end mode. Generated reads were mapped to the mouse (mm10) reference genome using TopHat v2.1.1 in combination with Bowtie2 ver. 2.2.8 and SAMtools ver. 0.1.18. For neonatal rat ventricular cardiomyocytes, sequencing was performed in a 101-base single-end mode and generated reads were mapped to the rat reference genome sequences (rn6). Fragments per kilobase of exon per million mapped fragments (FPKMs) were calculated using Cuffdiff 2.2.1. Raw data concerning this study was submitted under Gene Expression Omnibus (GEO) accession number GSE200667.

Hierarchical clustering was performed using Cluster 3.0<sup>28</sup> and JAVA Treeview.<sup>29</sup> Gene ontology analysis was performed using DAVID.<sup>30</sup> Pathway analysis was performed with iDEP (<http://ge-lab.org/idep/>). For upstream analysis of transcription factors, QIAGEN's Ingenuity Pathway Analysis was applied. Statistical thresholds were determined through the calculation of the activation z score of gene sets composed of randomly chosen perturbed genes with random sign of fold change that do not lead to significant results on average. (Ingenuity Downstream Effects Analysis, whitepaper). Adjusted p values (adj. Pval) and Activated z-scores were used to identify significant pathways and upstream regulators. The adj. P val indicates significance, while z-scores were used to define activation or inhibition. The strongest predicted activation corresponds to z scores  $\geq 2$ , and the strongest predicted inhibition corresponds to z scores  $\leq -2$ .

### Preparation of neonatal rat cardiac myocytes

Neonatal rat cardiac myocytes and non-myocytes were prepared from 1-day-old Wister rats. In brief, ventricles were incubated in 0.25% trypsin-EDTA solution (Gibco) for overnight at 4°C and then digested with collagenase type II (Worthington). The dispersed cells were then incubated in 10-cm culture dishes for 70 minutes to remove non-myocytes. The unattached viable cells were rich in cardiomyocytes (90–95%), and attached cells were used as non-cardiac myocytes fraction. All experimental procedures involving neonatal rats were approved by IACUC at Kansai Medical University (21–108).

### Cyclic stretch of cultured cardiac myocytes

Cardiac myocytes were seeded on stretch chambers coated with laminin (Invitrogen) and cultured for 3 days. Cells were then subjected to uniaxial cyclic stretch (20% in length, 30 cycles/minute) for 8 hours with cell stretch system (STB-1400-10; STREX, Japan).

### siRNA-mediated knockdown and Wnt5a stimulation

For *Wnt5a* and/or *Yap1* knockdown in cultured cardiac myocytes, siRNA was transfected using Lipofectamine RNAiMAX reagent (Invitrogen 13778150) approximately 60 hours before starting cyclic stretch. For *Wnt5a* stimulation, cells were treated with recombinant *Wnt5a* protein (100 ng/ml)<sup>13</sup> during 8 hours of stretch.

### Western blot analysis

Total protein was extracted and protein concentrations were measured using a BCA assay kit (Takara). Nuclear extract was prepared using Cell fractionation kit (CST #9038). The proteins were separated by SDS-PAGE and transferred to PVDF membranes. The membranes were blocked in 5% nonfat milk in TBST and incubated with diluted primary antibodies (1:1000) overnight at 4°C. After washing with TBST, the membranes were incubated with Horseradish peroxidase anti-rabbit (CST) secondary antibody for 2 hours at room temperature. Signals were detected with FUSION SOLOS (VILBER).

### Immunocytochemistry

Cells were fixed for 10 min at room temperature in PBS containing 4% (w/v) paraformaldehyde and permeabilized in PBS containing 0.1% (w/v) Triton X-100 and 3% (w/v) BSA for 10 min. Cells were incubated with primary antibodies overnight at 4°C. In case of unconjugated primary antibodies, cells were incubated with Alexa Fluor secondary antibodies (Invitrogen, 1:200) for 1 hour at room temperature. Images were obtained using a confocal microscope (LSM700, Carl-Zeiss, Jena, Germany).

### QUANTIFICATION AND STATISTICAL ANALYSIS

Data are shown as mean  $\pm$  SE. Statistical analysis were made by the non-parametric Mann-Whitney U test for 2 groups comparison or the ANOVA for more than three groups comparison. When appropriate, 2-way ANOVA followed by post-hoc tests were used for the comparison of four groups with two different interventions. Statistical significance was assumed if  $p < 0.05$ . All statistical analyses were performed with SPSS (Version 19.0, SPSS Inc).